Supplementary Material for:

How smooth is a dolphin? The ridged skin of odontocetes

Authors:

Dylan K. Wainwright[1], Frank E. Fish[2], Sam Ingersoll[1], Terrie M. Williams[3], Judy St. Leger[4],

Alexander J. Smits[5], George V. Lauder[1]

1. Supplementary methods

Animals were sampled at five different regions around the body:

1) Between the blowhole and the dorsal fin.
2) On the lateral surface of the dorsal fin at about midchord and midspan. (Beluga whales have no dorsal fin, so location was approximated).
3) On the lateral side of the body, ventral to the dorsal fin.
4) On the dorsal side of the flipper, at about midchord and midspan.
5) On the dorsal side of the fluke, at about midchord and midspan.

A fast-curing two-part silicone molding compound (RepliSet, Struers Inc.) was used to mold the surface of animals *in vivo* (Supplementary Figures 1-4). This molding compound has a reported resolution down to 0.1 µm (Struers, Inc.), can be applied quickly, and cures in 1-3 minutes. We applied the molding compound on a 2 cm by 2 cm skin patch at the five locations listed above to animals that were out of water during normal veterinary checkups (Supplementary Figures 1-4). The molding compound is non-toxic and skin-safe for mammals, and when molds were removed no residue remained on the skin.

Molds were prepared for casting by adhering them to a silicone mat and building a small lip around each mold using silicone aquarium sealant. Molds were then cast with a two-part Spurr low viscosity resin which cured in a lab oven (Supplementary Figure 5). The casts were then removed and were imaged using gel-based profilometry (GelSight Inc.). Gel-based profilometry works by pressing a gel disc with a painted bottom into a surface of interest and photographing the gel impression using six different lighting angles. The paint on the gel removes the effect of optical properties of the surface and the different lighting angles allow for surface topography to be reconstructed. These topographic three-dimensional images contain over 18 million three-dimensional points. Topographic images are analyzed in the program MountainsMap v7.4.8425 (Digital Surf, Besançon, France) where form is removed so that surface properties can be compared. This gel-based profilometry technique has been validated for animal skin surface measurement against known samples in our previous publications [1–3], and further comparative data are available in these references.

Using these topographic data we measured the surface metrology parameters root-mean-square roughness, skew, and kurtosis. Skew is a parameter that describes the distribution of heights on a surface – skew of zero indicates a normal distribution, negative skew indicates more valleys, and positive skew implies more peaks [4]. The equation for skew is as follows:

$$Skew = Ssk = \frac{1}{Sq^3} \iint_a (Z(x,y))^3 dxdy$$

Where *Z(x,y)* is the height of the surface relative to the mean surface height, *Sq* is the root-mean-square roughness, and *a* is the area of measurement. Kurtosis describes the distribution of extreme heights on a surface – values of three denote a normal distribution, values of less than three denote a lack of extreme high or low values, and values above three signify the presence of extreme low or high heights [4]. The equation for kurtosis is as follows:

$$Kurtosis = Sku = \frac{1}{Sq^4} \iint_a (Z(x,y))^4 dxdy$$

Odontocete cruising and sprinting speeds (Supplementary Table 1) were taken from a survey of literature that included observations of both captive and wild animals. Cruising speed was taken as a sustained regular swimming speed and sprinting speed was chosen as the highest reliable burst speed available for each species. In the case that multiple reliable values for either cruising or sprinting speed were found for a species, we averaged these values.

2. Roughness scaling and k+

If the flow over the dolphin is laminar, then we do not expect small roughness to affect the flow [5], except in so much as it might trip the boundary layer and cause it to become turbulent. For turbulent flow, however, we know that roughness effects can be very important [6]. Evidence suggests that dolphins have turbulent flow over their surface [7–9]. To determine if the flow over the surface is affected by roughness, we need to calculate the relative size of the roughness compared to the thickness of the viscous sublayer, that is, the parameter $k^+ = ku_\tau/\nu$. Here k is a characteristic roughness height, and ν is the kinematic viscosity of the fluid. The friction velocity u_τ is related to the local skin friction coefficient $C_f(x)$ at a distance x from the leading edge of the surface through the definition

$$\frac{u_\tau}{U_\infty} = \sqrt{\frac{C_f}{2}} \quad \text{and} \quad C_f = \frac{\tau_w}{\frac{1}{2}\rho U^2}$$

where U_∞ is the flow speed relative to the surface, ρ is the fluid density and τ_w is the viscous stress at the surface.

The value of the roughness parameter k^+ indicates the importance of roughness. According to the widely accepted criteria proposed by Nikuradse [6], for $k^+ < 5$ the surface is hydrodynamically smooth, and the roughness height has no effect on the frictional stress exerted by the flow on the surface, nor the velocity profile itself. In other words, the flow over surfaces with $k^+ < 5$ are indistinguishable from flows over completely smooth surfaces.

Estimating the value of k^+ requires some approximations since the state of the boundary layer on the dolphin is not known precisely. Using simple power law relationships, which ignore important effects like pressure gradient, curvature, three-dimensionality, we have [5,10,11]

$$C_f = \frac{0.0576}{Re_x^{0.2}}.$$

Here $Re_x = xU_\infty/\nu$ is the Reynolds number where ν is the kinematic viscosity of the fluid. Hence,

$$k^+ = 0.17\, Re_x^{0.9} \left(\frac{k}{x}\right).$$

For a given roughness height k at a given position, therefore, the largest value of k^+ will occur at the highest Reynolds number.

Here we will present an example calculation of k^+ for a bottlenose dolphin swimming at high speed. We will assume that for flow at x = 1 m (approximately where we see ridges on the dorsal surface of the bottlenose dolphin), we have $k = k_{max} = 9\times10^{-6}$ m, and $\nu = 10^{-6}$ m^2/s (seawater at about 15°C). If we take a sprinting speed of 9 m/s (Supplementary Table 1), then $Re_x = 9\times10^6$, $C_f = 0.0023$, and $k^+ = 2.8$. This value is not rough enough to effect the boundary layer flows here—Nikuradse suggests boundary flows can be affected above $k^+ = 5$ and Jiménez suggests it happens above $k^+ = 4$. In addition, our example is for the worst-case scenario (highest Reynolds number, largest measured ridge height for this species and region), and so for all other cases (and even this severe case) we expect roughness effects to be small or negligible.

These estimates depend on the approximations made here. However, even if x was halved, then k^+ would only be larger by about 7%. If, on the other hand, the speed was doubled then k^+ would be larger by 87% so that $k^+ = 5.1$. Unfortunately, there is no way to estimate how k^+ is changed when we neglect the effects of pressure gradient (largely favorable over the anterior portion of the body), streamline curvature (mostly convex over the anterior portion of the body), and streamline divergence, since such measurements do not exist.

References:

1. Wainwright DK, Lauder G V. 2016 Three-dimensional analysis of scale morphology in bluegill sunfish, *Lepomis macrochirus*. *Zoology* **119**, 182–195. (doi:10.1016/j.zool.2016.02.006)

2. Wainwright DK, Lauder G V. 2018 Mucus matters: the slippery and complex surfaces of fish. In *Functional Surfaces in Biology - From the Micro- to Nanoscale* (eds SN Gorb, E Gorb), pp. 223–246. Springer Berlin Heidelberg.

3. Wainwright DK, Lauder G V., Weaver JC. 2017 Imaging biological surface topography *in situ* and *in vivo*. *Methods Ecol. Evol.* **8**, 1626–1638.

4. Whitehouse DJ. 1994 *Handbook of Surface Metrology*. Philadelphia, USA: Institute of Physics Publishing.

5. Schlichting H, Gersten K. 2016 *Boundary-layer theory*. Springer.

6. Nikuradse J. 1933 *Strömungsgesetze in rauhen Rohren*. VDI-Verlag.

7. Fish FE, Rohr J. 1999 Review of dolphin hydrodynamics and swimming performance. *SPAWARS Syst. Cent. Tech. Rep. 1801, San Diego, CA.*

8. Fish FE, Legac P, Williams TM, Wei T. 2014 Measurement of hydrodynamic force generation by swimming dolphins using bubble DPIV. *J. Exp. Biol.* **217**, 252–260. (doi:10.1242/jeb.087924)

9. Lang AW, Jones EM, Afroz F. 2017 Separation control over a grooved surface inspired by dolphin skin. *Bioinspiration and Biomimetics* **12**, 1–35. (doi:10.1088/1748-3190/aa5770)

10. Jimenez J. 2004 Turbulent flows over rough walls. *Annu. Rev. Fluid Mech.* **36**, 173–196.

11. Smits AJ. 2000 *A physical introduction to fluid mechanics*. 1st edn. New York, New York, USA: John Wiley and Sons Inc.

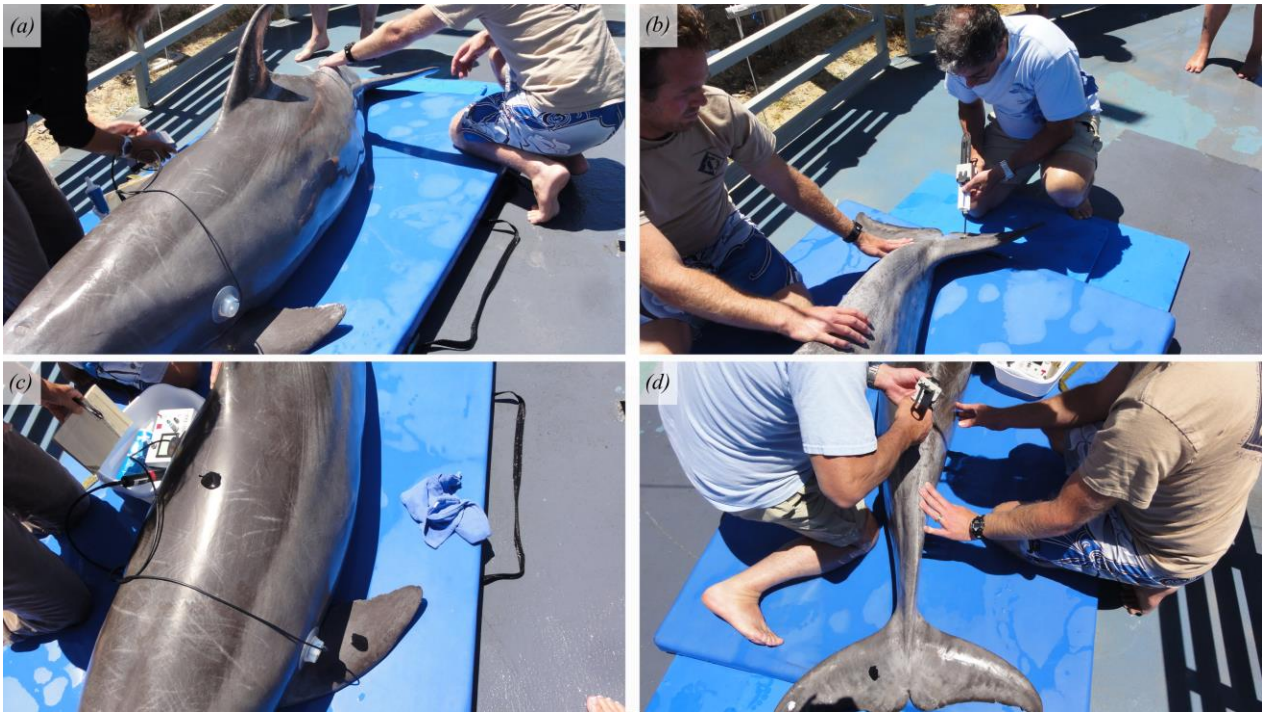

Supplementary Figure 1: Sampling skin texture of bottlenose dolphins. Animals were sampled during routine medical checks while out of water. Fast-drying molding compound (Repliset, Struers) was used to mold skin *in vivo*. (a) Preparation of an individual bottlenose dolphin at the University of California Santa Cruz. (b) Molding of skin texture on fluke (another view is shown in d and in supplementary figure 2b). (c) Molds curing on flipper and dorsal regions (molds are black material). (d) Mold shown curing on fluke as more molding compound is applied elsewhere.

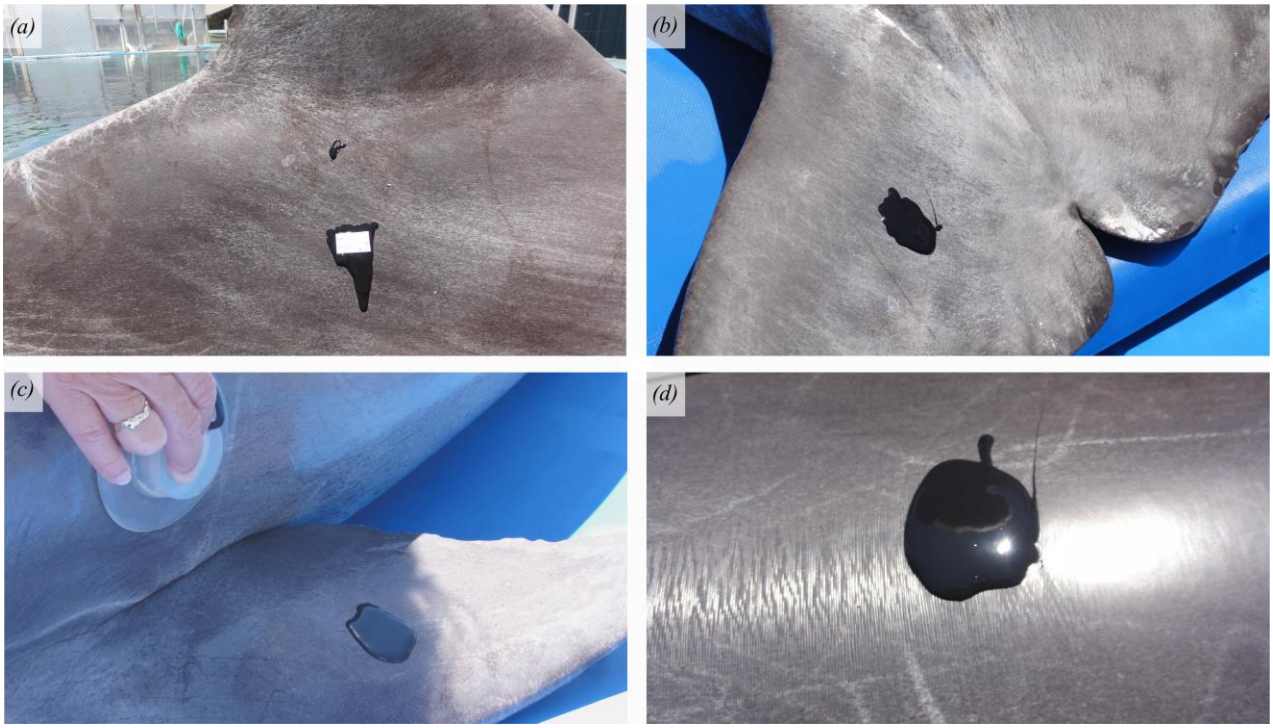

Supplementary Figure 2: Silicone molding compound applied to the skin of a bottlenose dolphin. (a) Lateral region below the dorsal fin. Molds were deliberately applied in an asymmetrical shape and pictures taken of each mold or a labeled tag adhered to the molds (as in panel a) to allow reconstruction of the orientation of the mold relative to the animal's long axis. (b) Closeup of silicone molding compound on fluke. (c) Mold applied to the flipper of a dolphin as heart rate is monitored. (d) Closeup of mold applied to dorsal region of a dolphin, between the blowhole and dorsal fin.

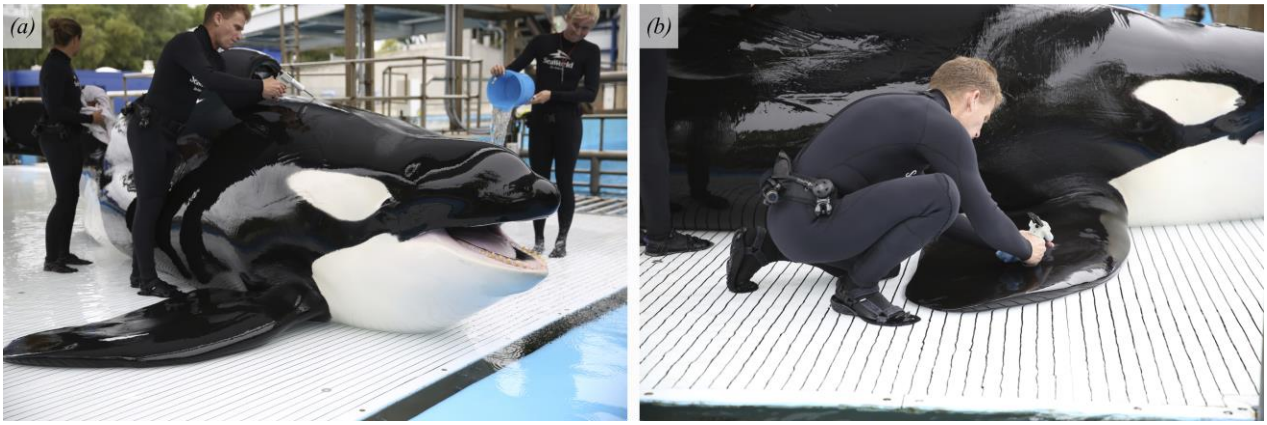

Supplementary Figure 3: (a) Molding of killer whale skin texture on the dorsal region, between the blowhole and dorsal fin. (b) Molding of the killer whale skin texture on the flipper.

Supplementary Figure 4: Molding of skin texture on white-sided dolphin and beluga whales. (a) Silicone molding compound applied to white-sided dolphin in relaxed position. (b) Molding applied to beluga whale. Black molding compound already curing on flipper. (c) Molding compound applied to beluga whale.

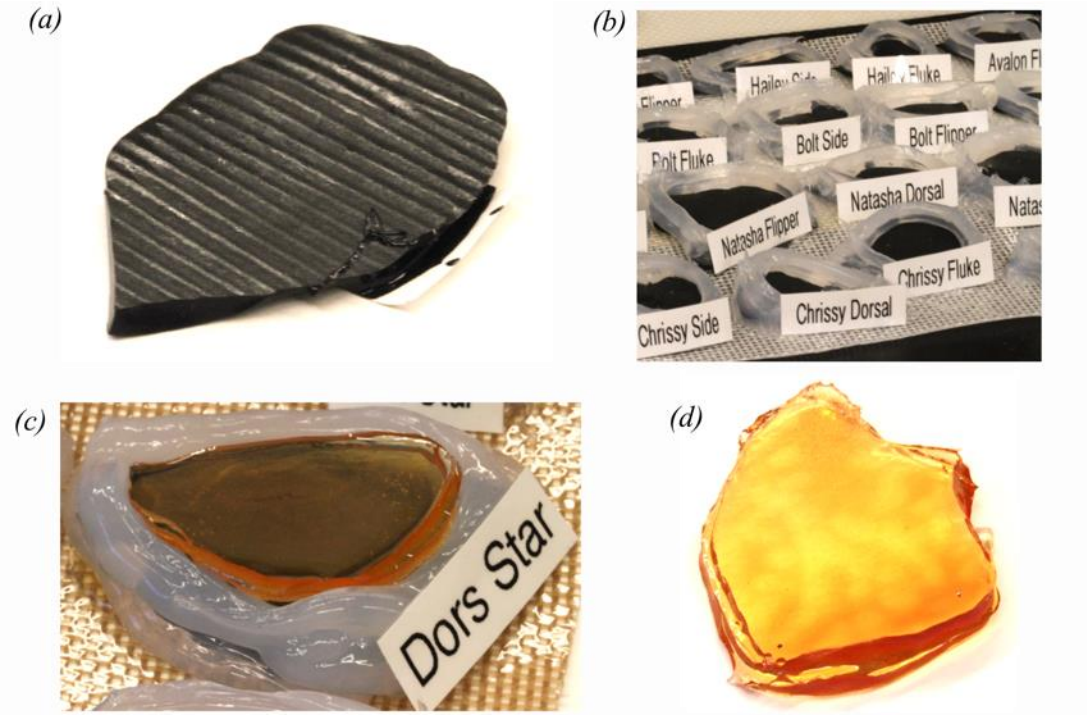

Supplementary Figure 5: Casting process. (a) Silicone mold with ridges. (b) Molds are labeled and lips are made so that molds can be cast. (c) Mold casted in two-part epoxy resin. (d) Mold removed and ready for surface profilometry.

2. Supplementary data

Below we show surface profilometry images from each location on each odontocete species studied.

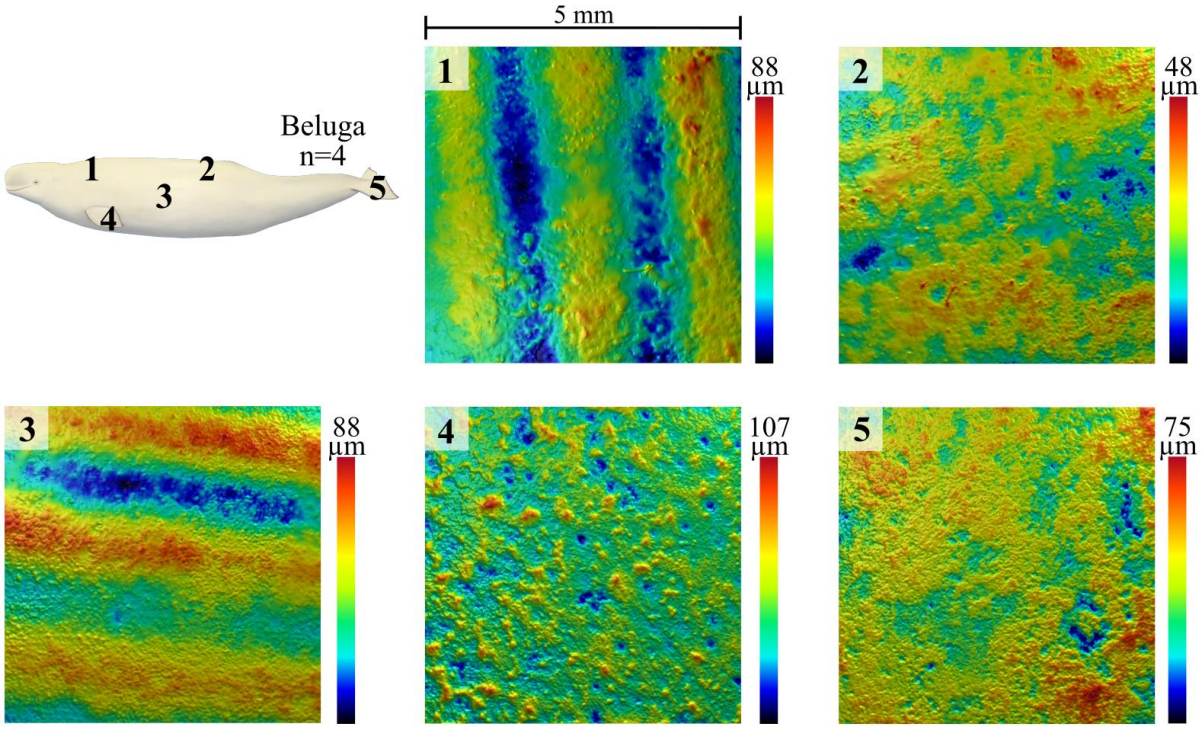

Supplementary Figure 6: Surface topography of beluga whales from five different regions. All surface image panels are 5 mm by 5 mm. Panels are oriented so that animal anterior is to the left. Each surface image has a different height scale, as given by colored scale bar at right.

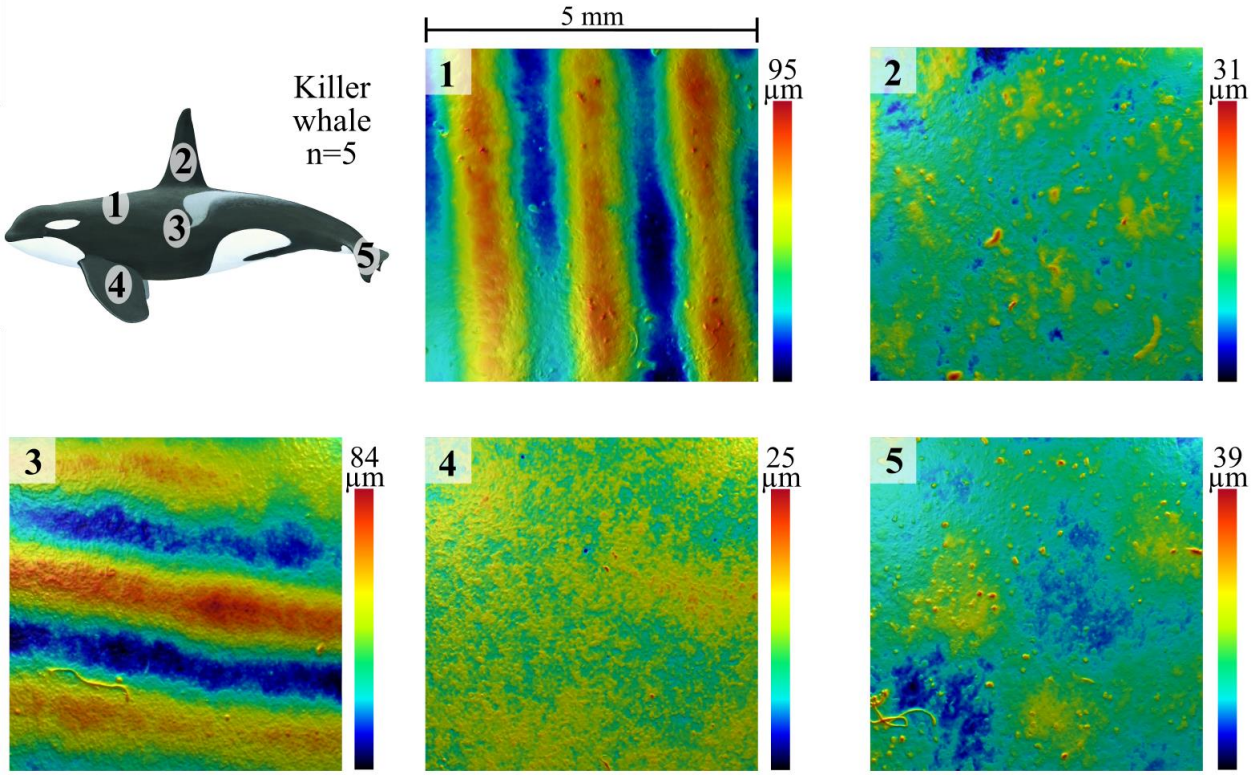

Supplementary Figure 7: Surface topography of killer whales from five different regions. All surface image panels are 5 mm by 5 mm. Panels are oriented so that animal anterior is to the left. Each surface image has a different height scale, as given by colored scale bar at right.

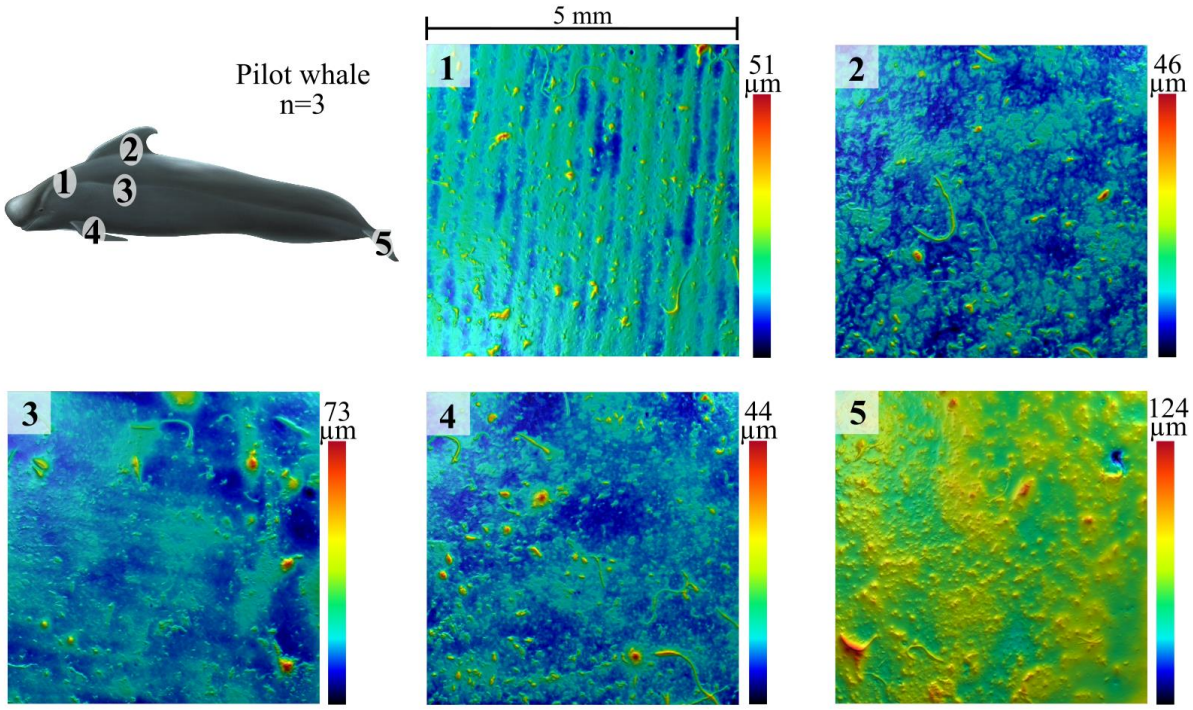

Supplementary Figure 8: Surface topography of pilot whales from five different regions. All surface image panels are 5 mm by 5 mm. Panels are oriented so that animal anterior is to the left. Each surface image has a different height scale, as given by colored scale bar at right.

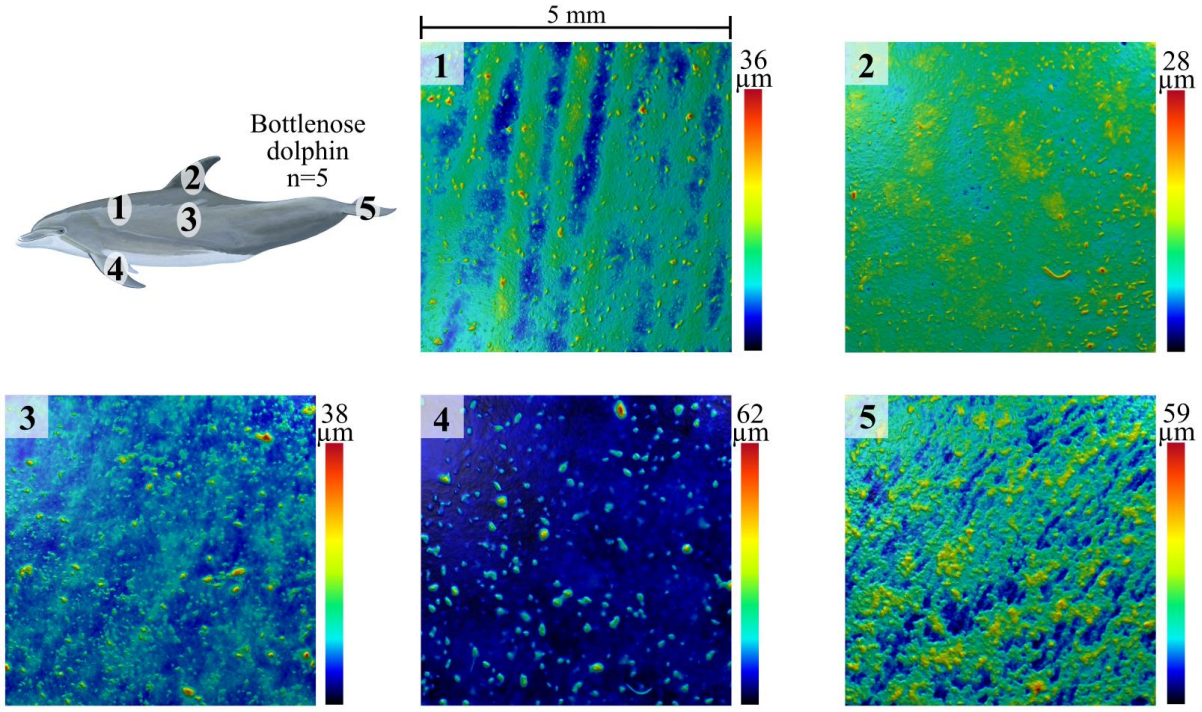

Supplementary Figure 9: Surface topography of bottlenose dolphins from five different regions. All surface image panels are 5 mm by 5 mm. Panels are oriented so that animal anterior is to the left. Each surface image has a different height scale, as given by colored scale bar at right.

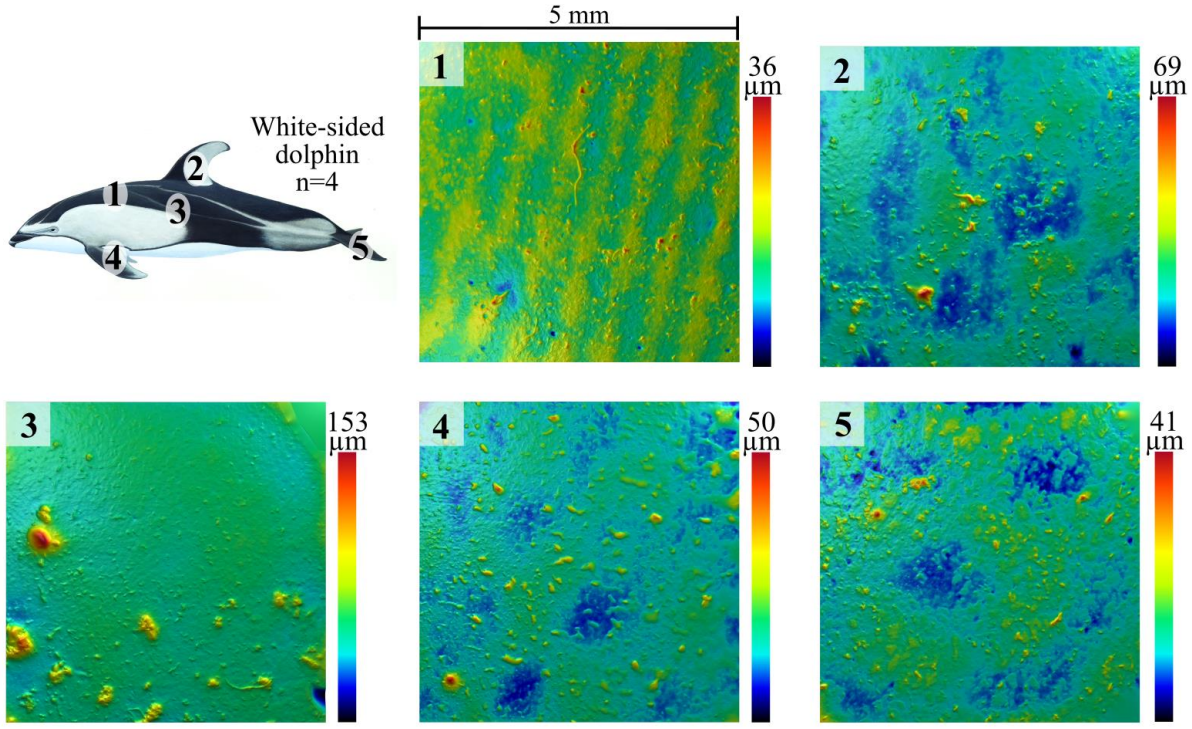

Supplementary Figure 10: Surface topography of white-sided dolphins from five different regions. All surface image panels are 5 mm by 5 mm. Panels are oriented so that animal anterior is to the left. Each surface image has a different height scale, as given by colored scale bar at right.

Supplementary Table 1: Cruising and sprinting speed used for each species.

Species	Cruise speed (m/s)	Sprint speed (m/s)
Bottlenose dolphin	1	9
White-sided dolphin	2	7
Pilot whale	2.5	9
Killer whale	1.7	10
Beluga whale	1.25	6

Supplementary Table 2: Length and weight for each individual sampled.
NA indicates that weights were not available for this individual.

Species	Length (m)	Weight (kg)
Bottlenose dolphin	2.9	239.5
Bottlenose dolphin	2.75	229.5
Bottlenose dolphin	2.413	176.5
Bottlenose dolphin	2.464	190.5
Bottlenose dolphin	2.96	319.3
White-sided dolphin	2.11	104.3
White-sided dolphin	2.159	124.7
White-sided dolphin	2	NA
White-sided dolphin	1.93	86.2
Pilot whale	4	NA
Pilot whale	4	NA
Pilot whale	4	NA
Killer whale	6	NA
Killer whale	6.22	4132.2
Killer whale	4.17	1174.8
Killer whale	5.18	2188.9
Killer whale	6.07	3265.9
Beluga whale	3.58	596
Beluga whale	3.78	1041.4
Beluga whale	3.54	635
Beluga whale	3.3	569.3

Supplementary Table 3: Percentage of the surface samples with ridges present in each species at each location for the individuals sampled in this study

Species	Location	Percent with ridges
Bottlenose dolphin	dorsal	100%
Bottlenose dolphin	dorsal fin	0%
Bottlenose dolphin	flipper	40%
Bottlenose dolphin	fluke	40%
Bottlenose dolphin	lateral side	20%
White-sided dolphin	dorsal	50%
White-sided dolphin	dorsal fin	0%
White-sided dolphin	flipper	0%
White-sided dolphin	fluke	0%
White-sided dolphin	lateral side	0%
Pilot whale	dorsal	100%
Pilot whale	dorsal fin	0%
Pilot whale	flipper	0%
Pilot whale	fluke	0%
Pilot whale	lateral side	33%
Killer whale	dorsal	100%
Killer whale	dorsal fin	0%
Killer whale	flipper	0%
Killer whale	fluke	0%
Killer whale	lateral side	100%
Beluga	dorsal	75%
Beluga	dorsal fin	0%
Beluga	flipper	0%
Beluga	fluke	0%
Beluga	lateral side	75%

Supplementary Table 4: Mean surface metrology metrics by species and location. Dashes for ridge height and wavelength indicate that this location lacked ridges.

Species	Location	Roughness (µm)	Skew	Kurtosis	Mean ridge height (µm)	Mean wavelength (mm)
Bottlenose dolphin	dorsal	1.99	1.87	14.80	5.86	0.50
Bottlenose dolphin	dorsal fin	2.04	2.85	27.36	-	-
Bottlenose dolphin	flipper	2.42	2.49	20.49	5.00	0.18
Bottlenose dolphin	fluke	4.09	1.11	22.45	9.03	0.17
Bottlenose dolphin	lateral side	2.66	4.74	54.34	2.67	0.63
White-sided dolphin	dorsal	4.01	0.90	9.25	11.77	0.63
White-sided dolphin	dorsal fin	3.14	1.67	15.74	-	-
White-sided dolphin	flipper	4.31	0.95	12.46	-	-
White-sided dolphin	fluke	3.30	1.28	11.26	-	-
White-sided dolphin	lateral side	5.00	2.66	21.21	-	-
Pilot whale	dorsal	3.42	2.13	19.12	5.58	0.23
Pilot whale	dorsal fin	4.74	3.51	29.60	-	-
Pilot whale	flipper	2.96	2.32	20.67	-	-
Pilot whale	fluke	4.15	1.87	15.34	-	-
Pilot whale	lateral side	4.81	3.11	26.07	3.77	0.30
Killer whale	dorsal	10.27	0.25	4.32	37.30	1.83
Killer whale	dorsal fin	2.73	1.22	10.89	-	-
Killer whale	flipper	3.98	0.72	9.06	-	-
Killer whale	fluke	3.32	1.29	15.74	-	-
Killer whale	lateral side	5.93	0.43	5.36	22.26	1.64
Beluga	dorsal	10.40	0.54	5.51	38.41	2.03
Beluga	dorsal fin	7.34	-0.29	4.57	-	-
Beluga	flipper	8.34	0.43	4.55	-	-
Beluga	fluke	7.49	0.13	4.63	-	-
Beluga	lateral side	21.70	-0.07	3.35	94.01	2.07